Spontaneous Motility of Actin Lamellar Fragments

C. Blanch-Mercader, J. Casademunt

Spontaneous Motility of Actin Lamellar Fragments

C. Blanch-Mercader and J. Casademunt

Departament d'Estructura i Constituents de la Matèria, Universitat de Barcelona, Avinguda Diagonal 647, E-08028 Barcelona, Spain

(Received 29 October 2012; published 15 February 2013)

We show that actin lamellar fragments driven solely by polymerization forces at the bounding membrane are generically motile when the circular symmetry is spontaneously broken, with no need of molecular motors or global polarization. We base our study on a nonlinear analysis of a recently introduced minimal model [Callan-Jones *et al.*, Phys. Rev. Lett. **100**, 258106 (2008)]. We prove the nonlinear instability of the center of mass and find an exact and simple relation between shape and center-of-mass velocity. A complex subcritical bifurcation scenario into traveling solutions is unfolded, where finite velocities appear through a nonadiabatic mechanism. Examples of traveling solutions and their stability are studied numerically.

DOI: 10.1103/PhysRevLett.110.078102 PACS numbers: 87.17.Jj, 47.20.Ky, 47.20.Ma, 87.17.Rt

Cell motility is deeply connected to spontaneous symmetry breaking and maintenance of functional asymmetry. In the context of actin-based motility of crawling cells, the transition from a roughly circular static cell to a motile cell has been an important focus of attention in recent years in experiments, theory and numerical simulation, in an effort to explain the shape of motile cells such as keratocytes and fibroblasts, and the mechanical mechanisms behind the complex actomyosin system that sustains motion [1–3]. Remarkably, fragments of cells that contain the actomyosin machinery but lack essential cell components, have also been shown to undergo such transitions to self-sustained motion [4,5]. It remains unclear, however, to what extent molecular motors and global polarization of such fragments are fundamental to achieve and sustain motion or, on the contrary, polymerization forces alone can couple to the shape providing a motility mechanism without an external or intrinsic symmetry breaking of the dynamics.

From a physical point of view, it is customary to construct minimal models of reduced complexity to elucidate the underlying mechanisms that connect shape to motion in such systems, and the role of the different biological ingredients that are present in real motile cells [6–9]. Within this spirit, a hydrodynamic approach based on the theory of active polar gels [10,11] has been proposed as a minimal model for cell lamellar fragments [12]. It has been shown that in the presence of high friction with the solid substrate, the actin gel dynamics can be approximated by a simple 2D Darcy flow, in similar conditions to viscous fingering in Hele-Shaw cells, a well-known paradigm of interfacial pattern formation [13–15]. However, the problem differs from viscous fingering in some fundamental aspects and thus it can be viewed also as a new prototype system in the context of Laplacian growth phenomena. In Ref. [12], it was found that actomyosin fragments do exhibit a viscous-fingering-like morphological instability, but the fundamental question of whether such a model contains the minimal ingredients to initiate and sustain motion remained unsolved. Extensions of this model to include an explicit symmetry-breaking of the dynamic equations to generate motility have also been reported [16]. Here we show that spontaneous symmetry breaking of the circular shape is sufficient to initiate and sustain motion, even in the absence of myosin motors and large-scale polarization, when nonlinearities are taken into account. We obtain an exact connection between geometry and kinematics of the fragments, showing that motile shapes are indeed generic. By means of conformal mapping techniques we unfold a complex bifurcation scenario in the transition from static to traveling states, where nonadiabatic effects confer a finite velocity to the traveling solutions.

Following Ref. [12], we describe a thin actin layer of actin cytoskeleton as an effective 2D single component, viscous fluid, bounded by a membrane with an arbitrary shape [11]. We assume that the relevant dynamics is sufficiently slow to neglect elastic effects. Actin is assumed to polymerize at the membrane, with a velocity v_p normal to it. Depolymerization is assumed to occur uniformly at a constant rate k_d in the fragment interior. Ignoring the dynamics of the actin polarization field as in Ref. [12], and assuming in addition that no myosin motors are present, the constitutive law reduces to that of an isotropic viscous fluid with viscosity η. Neglecting inertia, this leads to $-\boldsymbol{\nabla} P - \xi \mathbf{v} + \eta \Delta^2 \mathbf{v} = \mathbf{0}$, where P is the pressure and ξ is an effective friction coefficient. The velocity $\mathbf{v}$ can then be assumed to satisfy Darcy's law $\mathbf{v} = -M\boldsymbol{\nabla} P$ either because friction forces with the solid substrate dominate over viscous forces [12], implying $M = 1/\xi$, or more generally, by considering the actin layer to be in a confined geometry, for instance in a Hele-Shaw cell with a gap b. In this case, the standard averaging over the narrow third dimension yields $M = \frac{b^2}{12\eta} + \frac{1}{2\xi}$ [17]. The problem is thus reduced to a free-boundary problem for the boundary $\partial\Omega(t)$ of a 2D domain $\Omega(t)$. The flow equations of polymerized actin are nonconventional in two ways, namely,

the uniformly distributed sink that accounts for actin depolymerization in the bulk, and the existence of a line source localized at the boundary that accounts for actin polymerization, that is,

$$\nabla \cdot \mathbf{v} = -k_d, \tag{1}$$

$$V_n = \mathbf{v} \cdot \hat{\mathbf{n}} + v_p, \tag{2}$$

where the normal velocity of the interface V_n differs from the normal velocity of the fluid by the constant v_p, assuming that actin polarization is normal to the membrane [12]. In addition to the kinematic condition (2) that defines the motion of the boundary as part of the solution, we must supply a boundary condition for the pressure field. The simplest choice is to assume a Young-Laplace pressure drop across the membrane [12]. Neglecting the viscosity of the outer fluid this reads $P|_{\partial\Omega} = \gamma\kappa$, where κ is the curvature (taken positive for a circle) and γ is an effective surface tension.

The model can be transformed into the class of Laplacian growth problems by the change of variables $\mathbf{v}' = \mathbf{v} + k_d\mathbf{r}/2$ and $P' = P - k_d r^2/4M$. The free-boundary problem is thus fully specified by

$$\Delta P' = 0, \tag{3}$$

$$P'|_{\partial\Omega} = \gamma\kappa - \frac{k_d}{4M} r^2, \tag{4}$$

$$V_n = -\hat{\mathbf{n}} \cdot \left(M\nabla P' + \frac{k_d}{2}\mathbf{r} \right)|_{\partial\Omega} + v_p. \tag{5}$$

Equations (3) and (4) are formally identical to those corresponding to viscous fingering in a rotating Hele-Shaw cell [18]. The kinematic condition (5), however, defines a fundamentally different dynamics of the boundary, in particular restoring the translational invariance.

The linear stability analysis of a circle with radius $R_0 = 2v_p/k_d$ was studied in Ref. [12]. In the absence of molecular motors the growth rate of the m-fold sinusoidal perturbation reads $\lambda(m)k_d^{-1} = (m-1)/2 - \beta m(m^2-1)$, where $\beta \equiv \frac{M\gamma}{R_0^3 k_d}$ is a dimensionless parameter expressing the ratio of capillary to friction forces. A bifurcation occurs for those values of $\beta = \beta_n \equiv 1/[2n(n+1)]$, with $n > 1$, for which $\lambda(n) = 0$. It is worth stressing that, based on symmetry, this instability cannot generate motion at the linear level. In fact, only the mode $m = 1$ singles out a unique direction in space, corresponding to an infinitesimal shift of the circle. However, the mode $m = 1$ must be exactly marginal, $\lambda(1) = 0$, reflecting the translational invariance of the problem. Explicit symmetry breaking of the equations has been discussed as a possible mechanism to generate motion [16]. Here, we are interested in whether spontaneous symmetry breaking via a morphological instability is by itself sufficient to initiate and sustain motion, a fundamental question that must be addressed at the nonlinear level.

Before proceeding to a systematic nonlinear expansion, we report an exact result that relates kinematics and geometry in a remarkably simple and illuminating way. Consider the areal center of mass $R_A(t)$ of the domain $\Omega(t)$ of area $A(t)$ and the contour center of mass $R_L(t)$ of its boundary $\partial\Omega(t)$ of length $L(t)$. Using the exact equation

$$\frac{d}{dt} A(t) R_A(t) = \frac{d}{dt} \int_\Omega z\, da = \int_{\partial\Omega} z V_n\, dl, \tag{6}$$

where $z = x + iy$ is the complex variable, introducing Eq. (5) and (6), taking into account the mass balance relation $\dot{A} = v_p L - k_d A$, and using standard integral calculus, one can prove that [19]

$$\dot{R}_A = \frac{v_p L}{A}(R_L - R_A). \tag{7}$$

The separation between the two centers of mass is a measure of the asymmetry of the shape. According to Eq. (7), the system behaves effectively as driven by a flow from a point source to a point sink, located respectively at the geometric centers of polymerization and depolymerization. Such interplay between boundary and bulk differs fundamentally from other self-propulsion mechanisms reported in reaction-diffusion systems [20]. For any given shape, Eq. (7) gives us directly the velocity of the center of mass, so its trajectory is very simply encoded in the evolution of the shape. In particular, the existence of sustained locomotion with a finite velocity V_{st} is reduced to existence of asymmetric ($R_A \neq R_L$) stationary shapes, since Eq. (7) then reads $V_{\mathrm{st}} = k_d(R_L - R_A)$.

In order to describe the evolution of the shape we use conformal mapping techniques [13]. Without loss of generality, we take $R_0 = 1$ and we define $z = f(\omega, t) = \Sigma_0^\infty a_m(t)\omega^{m+1}$, with $\mathrm{Im}(a_0) = 0$, as an analytic function that maps the unit disk in the ω plane into the domain $\Omega(t)$ in the z plane. Then, Eqs. (3)–(5) can be shown to be equivalent to

$$\mathrm{Im}[\partial_\phi f \partial_t f^*] = \partial_\phi H_\phi \left[\frac{k_d}{4}|f|^2 - M\gamma\kappa[f] \right] + v_p|\partial_\phi f| - \frac{k_d}{2}\mathrm{Im}[f^*\partial_\phi f], \tag{8}$$

where the unit circle is $\omega = e^{i\phi}$, $\kappa[f]$ stands for the curvature, and H_ϕ denotes the Hilbert transform on the circle [19]. The shapes are conveniently parametrized with the set of complex amplitudes $a_m(t)$ which satisfy an infinite set of ordinary differential equations (ODEs) that follow from Eq. (8). An appropriate truncation of this set also defines a convenient numerical scheme to solve the evolution. This framework is particularly useful to extract the bifurcation structure of the system by means of the center manifold theorem [21] which formally decouples

the dynamics of the fast modes, with $\lambda(k) = O(1)$, from that of the slow modes, with $\lambda(n) = O(g_n)$ when $g_n \equiv \beta - \beta_n \ll 1$. Accordingly, close to each bifurcation β_n, the dynamics is topologically equivalent (i.e., homeomorphic) to a system with a closed set of nonlinear equations for the marginal modes, contained in an invariant manifold, and a linear dynamics for the fast modes. In our case, for $\beta \approx \beta_n$ and taking into account that $\lambda(1) = 0$ for any β, we have

$$\dot{a}_1 = N_{1n}[a_1, a_n, a_k(a_1, a_n)], \tag{9}$$

$$\dot{a}_n = \lambda(n)a_n + N_{nn}[a_1, a_n, a_k(a_1, a_n)], \tag{10}$$

$$\dot{a}_k = \lambda(k)a_k, \tag{11}$$

where k spans all nonnegative integers excluding 1 and n, and N_{1n} and N_{nn} are the nonlinear functions defined by the set of ODEs obtained from Eq. (8) [19]. The functions $a_k(a_1, a_n)$ define the so-called center manifold and can be obtained explicitly as power expansions around the bifurcation point following a standard procedure [21]. The amplitudes a_k in Eq. (11) stand for the transversal components to the center manifold.

It is worth remarking that Eq. (11) includes also unstable modes, which are not "slaved" to the slow modes. This fact is crucial to prove the nonlinear instability of the center of mass in our problem. In fact, the modes with $1 < k < n$ have $\lambda(k) > 0$ and have in general nonzero transversal components to the center manifold, which depart from it exponentially. For β_3, for instance, from the explicit form of Eqs. (9)–(11) and after writing $\dot{R}_A$ in Eq. (7) in terms of mode amplitudes, we find that the lowest order nonlinear coupling is $\dot{R}_A \sim a_2 a_3^*$. Consequently, the transversal components of these two modes lead to $\dot{R}_A \sim \exp\{[\lambda(2) + O(g_3)]t\}$, where $\lambda(2) = O(1) > 0$. This proves the nonlinear instability of the center of mass, a central result of this Letter. In addition, to prove that the motion of the center of mass will be sustained, it suffices to find stationary shapes with $R_A \neq R_L$, according to Eq. (7). Explicit stationary shapes can be obtained analytically near the bifurcation points in powers of g_n from the reduced nonlinear equations, Eqs. (9) and (10), and continued numerically away from the bifurcation. Here we focus on symmetry-breaking, motile shapes (subcritical bifurcations to nonmotile shapes are also found).

The order of expansion of the functions N_{1n} and N_{nn} that is required to fully unfold the nonlinear structure (i.e., the branches of solutions that bifurcate from the fixed point) is not known *a priori*. In our case, the fact that a_1 is strictly marginal introduces a high degeneracy into the problem. With the help of symbolic calculus software, we have explicitly determined Eqs. (9) and (10) to very high orders (up to 14) and we find that the number of branches bifurcating from the circle is consistently increasing with the order of expansion. A careful analysis of the behavior for increasing orders of the Newton polygon associated to this set of equations (analysis not shown) strongly suggests that the number of such branches could well be infinite. A typical branch of stationary solutions takes the form of an expansion such as

$$a_1^{\mathrm{st}} = 2\sqrt[4]{3}\, g_2^{1/4}[1 + O(g_2)], \tag{12}$$

$$a_2^{\mathrm{st}} = \frac{16}{\sqrt{3}} g_2^{1/2}[1 + O(g_2)], \tag{13}$$

$$A^{\mathrm{st}} = \pi + 8\pi g_2[1 + O(g_2)]. \tag{14}$$

Remarkably, however, V_{st} does not admit an expansion in powers of g_n. In fact, inserting the explicit solutions

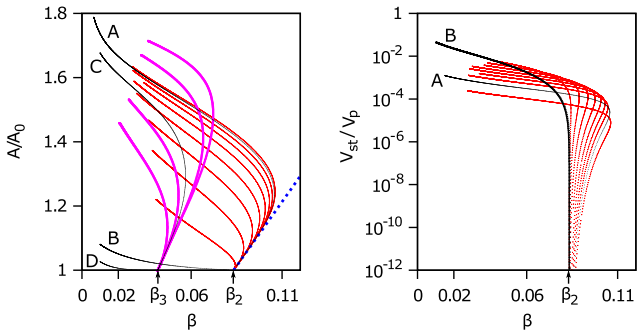

FIG. 1 (color online). Branches of stationary traveling solutions bifurcating from β_2 and β_3. Left: normalized area as a function of β, ($A_0 = \pi R_0^2$). Right: normalized velocity as a function of β. The dashed line is the common tangent to all branches at β_2, as defined by Eq. (14). Labels A, B, C, and D identify the branches plotted in Fig. 2.

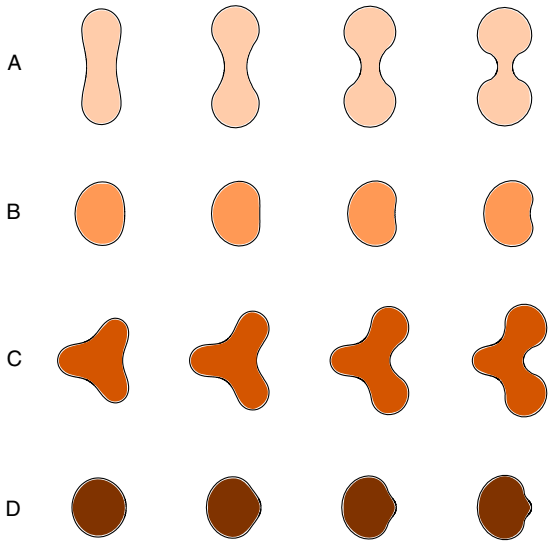

FIG. 2 (color online). Examples of stationary propagating shapes. A and B correspond to two branches bifurcating at β_2 and C and D at β_3, as defined in Fig. 1. β increases from right to left and velocity increases from left to right.

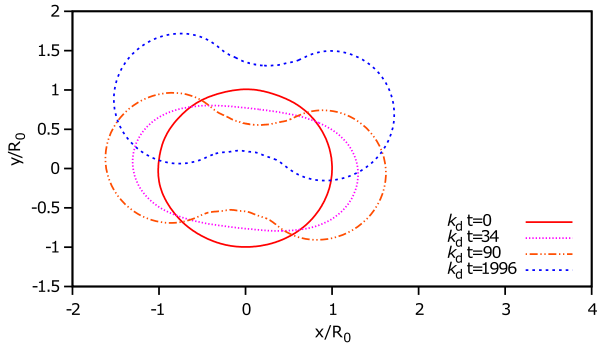

FIG. 3 (color online). Time evolution of a randomly perturbed circular interface for $\beta = 0.06$.

$a^{\mathrm{st}}_{1,2}(g_2)$ into the expression of V_{st} in Eq. (7) and using the center manifold relations $a_k(a^{\mathrm{st}}_1, a^{st}_2)$, we get an exact cancellation to all orders (explicitly checked up to order 14), suggesting that $V_{\mathrm{st}}(g_n)$ is exponentially small for $g_n \ll 1$ and cannot be obtained from the amplitude expansion. To pursue this puzzling point further, we have used extremely high-precision arithmetics (up to 64 digits) to obtain V_{st} numerically near the bifurcation point. Carefully analyzing the crossover towards an algebraic relaxation as a function of the order of truncation of the equations, we find that, for $g_2 \ll 1$, $V_{\mathrm{st}} = O(\exp(-a/g_2^{\nu}))$ with $a \approx 15.3$ and $\nu \approx 1/6$ (details not shown). Consequently, the mechanism to endow a given shape with a finite velocity appears to be nonadiabatic, i.e., a nonperturbative effect that is missed by the adiabatic (center manifold) reduction.

In Fig. 1, we plot some of the stationary branches obtained numerically, and their propagation velocity, using continuation techniques away from the bifurcations β_2 and β_3 (see corresponding shapes in Fig. 2). Note that all branches are subcritical. In addition, we have numerically checked the linear stability of some of the nonlinear traveling solutions obtained. We find that the two solutions branching from β_2 labeled as A and B in Figs. 1 and 2, are indeed linearly stable. However, it is plausible to expect that the majority of the branches will be unstable and hence essentially unobservable. Finally, we have integrated the full time-dependent evolution from a circular interface under random, small perturbations and find that the peanut-shaped branch (row A of Fig. 2) exhibits a seemingly large basin of attraction, including all cases of perturbed circles that we have checked out. A typical evolution is shown in Fig. 3.

In conclusion, we have shown that actin polymerization forces combining localized assembly at the boundary and distributed disassembly in the bulk, together with friction with the environment, are sufficient to initiate and sustain motion of actin fragments through a nonlinear morphological instability mechanism. Consequently, spontaneous motility does not necessarily require molecular motors, large-scale actin polarization, intrinsic symmetry breaking, or any type of biochemical regulation, even though all these ingredients are usually present and do enhance the motility of real fragments and cells. We have thus identified a minimal mechanism of spontaneous motility that underlies and may have preceded the very complex actin-based machinery optimized by evolution. Several effects disregarded in our analysis may take over after the initial instability and modify the dynamics, so the shapes and velocities here obtained must be seen as a proof of principle, not as a quantitatively accurate description of actual fragments and cells. Nevertheless, to the extent that the Darcy flow regime stands, the model can be extended to include more general boundary conditions at the membrane, molecular motors, external forces, and also inhomogeneous parameters k_d, v_p, or γ, allowing for more realistic dynamics and shapes. In particular, Eq. (7) can be generalized and becomes a useful test to relate simple direct observables, such as shape and velocity, to the different dynamical ingredients. For instance, relaxing the assumption of normal polarization of actin at the membrane, which is often violated in real systems with the formation of rear actin cables [4], we may admit an arbitrary polarization $\mathbf{p}$ at the boundary, with $V_n = (\mathbf{v} + v_p\mathbf{p}) \cdot \hat{\mathbf{n}}$. Then, Eq. (7) takes the form of the contour average $A\dot{R}_A = v_p L\langle (z - R_A)(\mathbf{p} \cdot \hat{\mathbf{n}})\rangle_L$, which yields more realistic values of V_{st}, of the order of v_p, for the typical crescent shapes and polarization at the boundary observed in real fragments.

As a final remark, it is worth stressing that, in addition to its biological relevance, the model here studied is interesting from a physical point of view as a new prototype within the class of Laplacian growth problems in interfacial pattern formation [13–15], and in the context of self-propelled systems under nonequilibrium conditions (see Ref. [20] and references therein).

We thank A. Jorba and C. Simó for illuminating discussions on the mathematical subtleties of this problem and for help in the use of very high-precision arithmetics. We acknowledge financial support under Projects No. FIS2010-21924-C02-02 and No. 2009-SGR-014. C. B.-M. also acknowledges a FPU grant from the Spanish government.

[1] P. T. Yam, C. A. Wilson, L. Ji, B. Hebert, E. L. Barnhart, N. A. Dye, P. W. Wiseman, G. Danuser, and J. A. Theriot, J. Cell Biol. **178**, 1207 (2007).

[2] C. A. Wilson, M. A. Tsuchida, G. M. Allen, E. L. Barnhart, K. T. Applegate, P. T. Yam, L. Ji, K. Keren, G. Danuser, and J. A. Theriot, Nature (London) **465**, 373 (2010).

[3] K. Keren, Z. Pincus, G. M. Allen, E. L. Barnhart, G. Marriott, A. Mogilner, and J. A. Theriot, Nature (London) **453**, 475 (2008).

[4] A. B. Verkhovsky, T. M. Svitkina, and G. G. Borisy, Curr. Biol. **9**, 11 (1999).
[5] M. F. Fournier, R. Sauser, D. Ambrosi, J.-J. Meister, and A. B. Verkhovsky, J. Cell Biol. **188**, 287 (2010).
[6] K. Doubrovinski and K. Kruse, Phys. Rev. Lett. **107**, 258103 (2011).
[7] D. Shao, W. J. Rappel, and H. Levine, Phys. Rev. Lett. **105**, 108104 (2010).
[8] F. Ziebert, S. Swaminathan, and I. S. Aranson, J. R. Soc. Interface **9**, 1084 (2012).
[9] D. Shao, H. Levine, and W.-J. Rappel, Proc. Natl. Acad. Sci. U.S.A. **109**, 6851 (2012).
[10] K. Kruse, J. F. Joanny, F. Jülicher, J. Prost, and K. Sekimoto, Eur. Phys. J. E **16**, 5 (2005).
[11] F. Jülicher, K. Kruse, J. Prost, and J. Joanny, Phys. Rep. **449**, 3 (2007).
[12] A. C. Callan-Jones, J. F. Joanny, and J. Prost, Phys. Rev. Lett. **100**, 258106 (2008).
[13] D. Bensimon, L. Kadanoff, S. Liang, B. Shraiman, and C. Tang, Rev. Mod. Phys. **58**, 977 (1986).
[14] J. Casademunt and F. X. Magdaleno, Phys. Rep. **337**, 1 (2000).
[15] J. Casademunt, Chaos **14**, 809 (2004).
[16] M. Ben Amar, O. V. Manyuhina, and G. Napoli, Eur. Phys. J. Plus **126**, 19 (2011).
[17] R. J. Hawkins, M. Piel, G. Faure-Andre, A. Lennon-Dumenil, J. Joanny, J. Prost, and R. Voituriez, Phys. Rev. Lett. **102**, 058103 (2009).
[18] L. Carrillo, F. X. Magdaleno, J. Casademunt, and J. Ortin, Phys. Rev. E **54**, 6260 (1996).
[19] See Supplemental Material at http://link.aps.org/supplemental/10.1103/PhysRevLett.110.078102 for details of the derivation of Eqs. (7)–(10).
[20] K. Shitara, T. Hiraiwa, and T. Ohta, Phys. Rev. E **83**, 066208 (2011).
[21] J. D. Crawford, Rev. Mod. Phys. **63**, 991 (1991).